Climatically driven emissions of hydrocarbons from marine sediments during deglaciation

T. M. Hill*[†], J. P. Kennett*[‡§], D. L. Valentine*, Z. Yang*, C. M. Reddy[¶], R. K. Nelson[¶], R. J. Behl[∥], C. Robert**, and L. Beaufort**

*Department of Earth Science and Marine Science Institute, University of California, Santa Barbara, CA 93106; [¶]Marine Chemistry and Geochemistry Department, Woods Hole Oceanographic Institution, MS No. 4, Woods Hole, MA 02543; [∥]Department of Geological Sciences, California State University, 1250 Bellflower Boulevard, Long Beach, CA 90840; and **Centre Européen de Recherche et d'Enseignement des Géosciences de l'Environnement, Unité Mixte de Recherche 6635, Centre National de la Recherche Scientifique, Europole Mediterraneen de l'Arbois, BP80, 13545 Aix-en-Provence Cedex 4, France

Marine hydrocarbon seepage emits oil and gas, including methane ($\approx$30 Tg of CH_4 per year), to the ocean and atmosphere. Sediments from the California margin contain preserved tar, primarily formed through hydrocarbon weathering at the sea surface. We present a record of variation in the abundance of tar in sediments for the past 32,000 years, providing evidence for increases in hydrocarbon emissions before and during Termination IA [16,000 years ago (16 ka) to 14 ka] and again over Termination IB (11–10 ka). Our study provides direct evidence for increased hydrocarbon seepage associated with deglacial warming through tar abundance in marine sediments, independent of previous geochemical proxies. Climate-sensitive gas hydrates may modulate thermogenic hydrocarbon seepage during deglaciation.

methane | paleoclimate | Quaternary climate | hydrate | tar

Dramatic changes in atmospheric methane concentrations have occurred on glacial–interglacial and millennial time scales and are typically attributed to varying biological production of CH_4 in wetlands (1). However, contributions from "geologic" methane sources, including thermogenic hydrocarbons in hydrates and/or sedimentary reservoirs, remain largely unknown. Quantifying past and present emission rates of methane from marine and terrestrial hydrocarbon sources is critical in understanding the contribution of methane to the atmosphere from these natural sources (2, 3).

Marine hydrocarbon seepage emits oil and gas, including methane ($\approx$30 Tg of CH_4 per year globally), to the ocean and atmosphere (3). In the southern California region, >200 persistent hydrocarbon seeps have been reported, with several in Santa Barbara Channel (SBC) (Fig. 1). Seepage in this region is controlled by faults and anticlines overlying a reservoir of thermogenic hydrocarbons derived primarily from the Monterey Formation, which is the source and reservoir rock (4). Most identified seeps in this region are located at shallow water depths (20–60 m), but locations of active seepage and seepage "indicators" (pockmarks, mud volcanoes, and tar mounds) have also been identified between 300 and 590 m (Fig. 1) (5, 6). At modern seeps in SBC, all observed petroleum seepage is closely associated with gas emission; in fact, seepage of methane gas far exceeds that of petroleum (8, 9). Although there is significant tar/hydrocarbon accumulation at localized sites of seepage, surface-ocean oil slicks can extend for >10 km from their source in the SBC region (2, 8, 9). Because oil at the sea surface is biologically degraded and volatile components evaporate, a negatively buoyant tar residue forms, which is eventually deposited on beaches and in basin sediments (2). However, general observations indicate little or no long-term accumulation of tar on these beaches, because the tar is removed from the shoreline within the timescale of tidal cycles.

In the SBC region, existing sediment geochemistry records, pockmark ages, and changing geochemical composition of fault–vein calcites provide evidence for variable hydrocarbon emissions during the late Quaternary (10–13). Negative $\delta^{13}C$ shifts recorded in planktonic foraminifera during rapid interstadial warming events in SBC have been interpreted as destabilization of methane hydrates and release of methane to the water column and atmosphere (11). In addition, $\delta^{13}C$ values and radiocarbon dating of foraminifera from a pockmark near modern seeps in SBC suggest gas emissions during the last 25,000 years (25 ky) (12). U-Th dating and $\delta^{13}C$ composition of fault vein calcites indicate intermittent hydrocarbon seepage in this area for the past $\approx$500 ky (10). Sediments from Ocean Drilling Program (ODP) Site 1016, offshore Point Conception (northwest of SBC), record changing concentrations of petroleum compounds over the past 150 ky (13). This record indicates an increase in petroleum compounds (hopanes) preserved in offshore sediments during major deglacial warming episodes (13). Collectively, these records suggest that hydrocarbon seepage on the California margin has been variable during the late Quaternary. We employ changing abundance of tar in marine sediments as a direct proxy for hydrocarbon seepage in the latest Quaternary.

The SBC overlies the northernmost physiographic basin of the California Continental Borderland. The 590-m-deep Santa Barbara Basin is bounded by a deep western and shallower eastern sill and encompasses nearly 5,000 km². A persistent gyre dominates the western end of the channel for much of the year, influenced by short-term upwelling and the southward-flowing California Current and opposing Southern California Countercurrent. The cores studied in this investigation were taken from the *R/V Marion Dufresne*, in the central basin (569 m) and the eastern end of the basin (481 m; Fig. 1). Sedimentation rates at these locations were relatively high and constant for the past $\approx$30 ky, averaging 130 cm/ky.

Results

Marine sediments are routinely microscopically examined to investigate the sand-sized fraction, including microfossils. While investigating rapid climate change in cores from SBC, we observed variable abundances of tar in the sedimentary record. To quantify the occurrence of tar, an index was established to reflect the percent of sand grains (>63 μm) observed under light
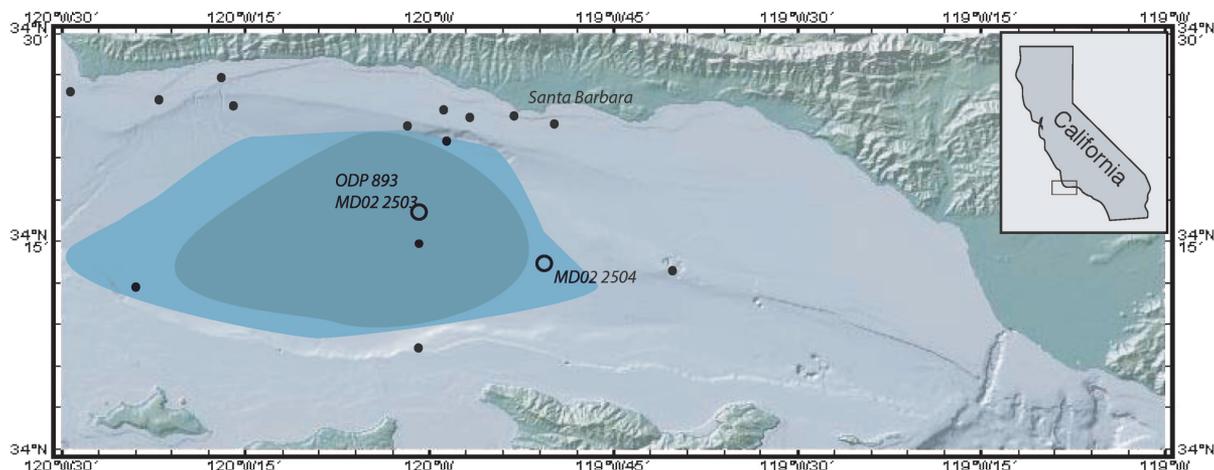
Fig. 1. Map of SBC indicating MD02-2503 (570 m; 34.28N, 120.04W, adjacent to ODP Site 893) and MD02-2504 (440 m; 34.23N, 119.86W) coring sites (open circles), collected in June 2002 from the *R/V Marion Dufresne*. Sedimentation rates at these locations averaged 130 cm/ky. The location of previously described methane seepage sites (from hydrocarbon or gas hydrate reservoirs) are indicated by black circles; these seepage sites were inferred by the identification of active gas seepage, tar mounds, mud volcanoes, pockmarks, and/or authigenic carbonates, sometimes accompanied by *Beggiatoa*-like organisms (sulfide-oxidizing bacteria); seepage sites were summarized from refs. 4–6. Areas of the gas hydrate stability zone are shaded for the Last Glacial Maximum and the Holocene (light blue-gray shading) and Termination IA (dark gray shading). Explanation of these scenarios and the estimates of gas hydrate stability are presented in the discussion and in Fig. 4. The total area of gas hydrate stability decreased during deglaciation, potentially destabilizing hydrates shown in the lighter blue-gray region. Map was adapted from refs. 4, 6, and 7 and GeoMapApp (www.marine-geo.org/geomapapp).

microscopy composed of and/or covered by tar (Fig. 2). The quantitative visual analysis and generation of the "tar index" was then used to target specific intervals for additional analyses. As such, variations in the weight percent of tar were determined in selected samples by means of solvent extraction (for methods, see *Supporting Text* and Table 1, which are published as supporting information on the PNAS web site). The tar index was preferred over gravimetric analysis for the following reasons: it is less labor intensive and allows for greater sampling frequency, it is nondestructive, and it provides immediate integration of tar observations with other sedimentary parameters. Although hydrocarbon emissions are subject to dispersal and degradation, the tar index utilizes the fraction of hydrocarbons that remain preserved in the geologic record. In addition to the quantitative tar index, tar from seven sediment samples was combined and analyzed by using comprehensive two-dimensional gas chromatography (GCxGC), which confirmed that it is similar to tar found on modern Santa Barbara beaches (see Fig. 5, which is published as supporting information on the PNAS web site) (9).

A planktonic foraminiferal (*Globigerina bulloides*) δ^{18}O record for both cores is presented for climatic context. The chronology of both cores is based on multiple correlations to the established record at ODP Site 893 (Fig. 2) (14).

The tar index (Fig. 2) reflects varying abundance of tar in SBC sediments over the last 32 ky. A "background" abundance (Index 1–2) of tar is apparent, consistent with modern observations of persistent hydrocarbon seepage. The abundance of tar in MD02-2503 increased during several intervals. Tar abundance episodically increased from 31,000 years ago (31 ka) to 26 ka, in association with the stadial/interstadial climatic instability of Marine Isotope Stage 3, as apparent in the δ^{18}O record. Distinct increases are observed again from 16.2 to 14.2 ka, coincident with deglacial warming and the onset of the Bølling–Allerød chronozone (B/A); this interval includes the greatest tar abundance ($\approx$15–14 ka). Finally, tar abundance increased again over the transition into the early Holocene ($\approx$11 ka). The tar index record for MD02-2504 exhibits similar tar abundance oscillations, with increased tar before and during Termination IA (16–14 ka) and again over Termination IB (11–10 ka). In both

cores, the tar index indicates decreased tar abundance during the Holocene compared with the glacial termination.

Discussion

We interpret the tar investigated in this study as reflecting hydrocarbon weathering and deposition that is synchronous with the sedimentation at the core sites, not seepage that has migrated upward through the sedimentary column. Several lines of evidence support this interpretation. First, as discussed above, petroleum from the Monterey Formation that floats to the surface is readily weathered in oil slicks to the point of becoming negatively buoyant, presumably because of its unusually high resin, asphaltene, and heteroatom content (2, 17). Consistent with this observation, hydrocarbon compounds have been detected in sinking particles collected in sediment traps in Santa Barbara Basin (18). This mechanism provides the source for tar throughout the SBC, including shoreline and deeper basin sediments. Second, there is no indication that changes in characteristics of the sedimentary record correlate with changes in the tar index. For example, changes in lamination/bioturbation of SBC sediments are not associated with tar index variability; rather, a distinct delay exists ($\approx$2 ka) between the timing of increased tar index values and the onset of laminations during deglaciation. This observation rules out a sedimentary-driven process, such as an increase in lamination strength providing a "seal" for upward migration of hydrocarbons. Finally, regardless of tar index values, the tar was consistently observed accreting to regular marine sedimentary material, including pelagic biogenic components, suggesting that the tar was deposited contemporaneously with these sediments.

We interpret the variations in the relative abundance of tar as a proxy for changing emissions of hydrocarbons, including methane. As stated previously, methane gas emission is closely associated with petroleum seepage in SBC (8, 9). In turn, variability of active hydrocarbon fluid flow has been inferred previously from fault calcites in the Santa Barbara region over the past 500 ka (10). These observations are consistent with our interpretations of variability in hydrocarbon seepage in this region. Based on the tar index, hydrocarbon emissions clearly increased during deglacial warming (16–14 ka and 11–10 ka; Fig.
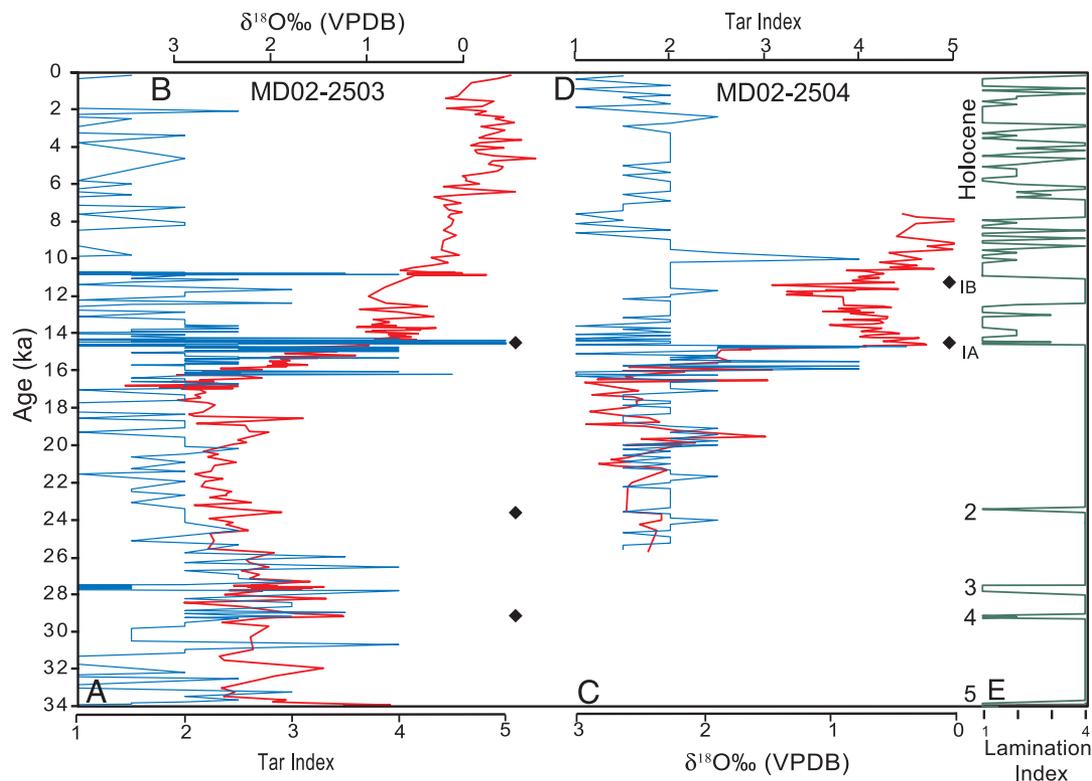
Fig. 2. Tar index records from SBC, compared with δ¹⁸O and lamination strength. (*A*) Tar index (blue) for MD02-2503. (*B*) δ¹⁸O of *G. bulloides* (red) for MD02-2503. (*C*) δ¹⁸O of *G. bulloides* (red) for MD02-2504. (*D*) Tar index (blue) for MD02-2504. Tar index reflects the % of sand grains composed of or coated by tar (e.g., 1 = 10%, 5 = 50%). (*E*) Lamination index for MD02-2503 (1, well laminated; 4, massive/bioturbated). The lamination index has been shown to change in concert with climatic changes recorded in the Greenland ice core (GISP2) (15). Isotopic data are from ref. 16. Location of chronological tiepoints (to ODP 893) (14) are denoted by diamonds. Major climatic intervals (Holocene, Terminations IA and IB) as well as Interstadials 2–5 are labeled.

2). In contrast, the Holocene exhibits relatively low hydrocarbon emission rates. Although increased variability in seepage was associated with Marine Isotope Stage 3, the most conspicuous hydrocarbon emissions occurred during the abrupt climate changes of Terminations IA and IB.

Many previous investigations of seepage in this region have focused on shallow water depths (20–60 m). These seepage sites are too shallow to contribute to the tar index record, which indicates increased hydrocarbon seepage during early deglacial warming, when sea levels were >100 m lower. However, locations of active seepage and seepage "indicators" have been identified in the modern basin between 300 and 590 m (Fig. 1) (5, 6). These observations provide ample evidence for seepage sites within the depth range required to explain the tar index record. In addition, hydrocarbon deposits are common along the California coast, and the tar index may incorporate hydrocarbons originating from outside of SBC (19). Comparison of the tar index between the two cores indicates that the deeper site (MD02-2503) has higher index values during the deglacial episode. This result may reflect location of seepage sites or that basin circulation acted to focus tar at the central site.

We consider several mechanisms that could change seepage rates and/or accumulation of hydrocarbons. Sea level could potentially affect the locations and rate of seepage: during lower sea level of the last glacial, marine seepage might have increased because of reduced hydrostatic pressure at the sediment–water interface and exposure of seeps on continental shelves (20). This process has been observed on short time scales: Hydrocarbon seepage rates in the SBC are partially controlled by changes in hydrostatic pressure during tidal cycles (21). However, sea level could not have been the primary mechanism that controlled past

hydrocarbon emissions because the deglacial transgression was a time of increasing tar abundance in basin sediments. Alternatively, sea-level rise and transgression may have "activated" shallow seepage sites by reconnecting them with the ocean; however, sea-level curves indicate only modest sea-level rise (15–20 m) from 19 to 14.6 ka, with much of the sea-level change following the abrupt deglacial warming (22). Thus, sea level apparently did not play an important role in increasing hydrocarbon emissions during the deglaciation. Increased storminess during deglaciation may have mobilized existing tar deposits; however, there is no sedimentologic evidence for these processes, such as the presence of sand layers (23). The restriction of the basin because of lowered sea level may have acted to concentrate tar deposition near the basin center, but this alone is unlikely to account for a 3-fold increase in percent tar (Fig. 3) or for the association with deglaciation. Therefore, we look for mechanisms beyond sea level, remobilization of hydrocarbon deposits, and basin restriction to explain the deglacial increase in tar abundance.

The increase in tar abundance may reflect subsurface interaction between thermogenic hydrocarbons and methane hydrate, which is widely present on continental margins, dependent on water temperature, pressure, and the presence of thermogenic or biogenic methane (Fig. 4) (24). Gas hydrates commonly overlie or occur near thermogenic reservoirs, such as in the Gulf of Mexico and the western margin of North America, with subsurface connectivity between the reservoirs (25, 26). Therefore, factors influencing the stability of hydrates could influence thermogenic hydrocarbon migration. We suggest that hydrate instability, which may be sensitive to Quaternary climate change, modulated hydrocarbon fluxes by means of several potential mechanisms: the upward migration of hydrocarbons through
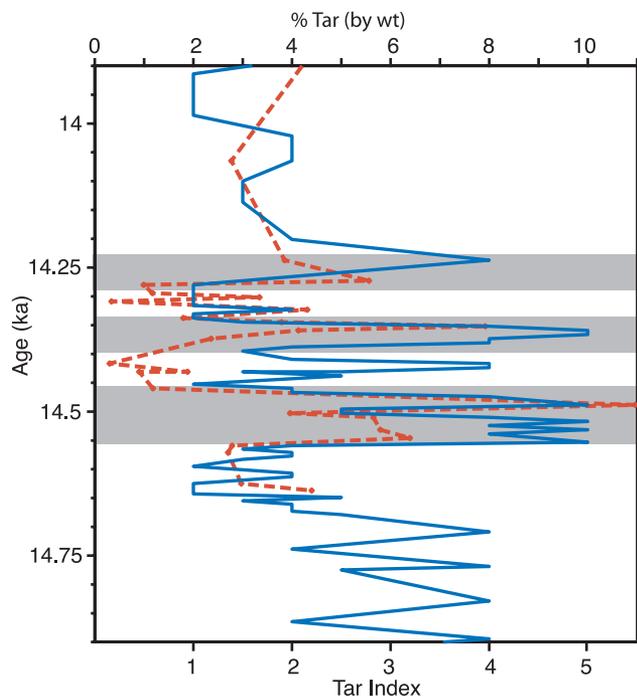
Fig. 3. The tar index (blue) and weight % tar (red, dashed line) covary in MD02-2503 between 15 and 14 ka. Three distinct pulses (shaded) of tar abundance are recorded by the tar index and % tar, reaching maximum values of 4–5 in the tar index and 5–11% by weight (a 3-fold increase from background values).
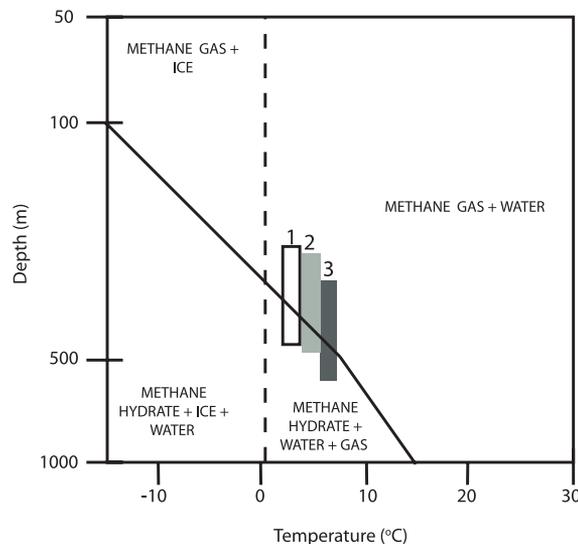

Fig. 4. Idealized gas hydrate stability model for the SBC during three separate intervals of the past ≈25,000 years. Each box is of equal size, representing the deepest 250 m of the SBC. Scenarios refer to those described in *Discussion* and shown in Fig. 1. Scenario 1: Last Glacial Maximum (18 ka), with maximum basin depth of ≈470 m and bottom water temperatures of 2°C. Scenario 2: Termination IA (16–14 ka), when bottom water temperatures had warmed by ≈2°C and sea level had risen by only 15m (maximum basin depth 485 m) (22). Scenario 3: early Holocene (≈9 ka), with basin near modern depth of 590 m; bottom waters had warmed by an additional 1-2°C. During scenarios 1 and 3, almost half of the deep SBC waters were within the gas hydrate stability field, promoting instability of gas hydrates at shallower depths. This figure highlights the importance of temperature change (relative to sea level) in gas hydrate stability. Gas hydrate stability curve was adapted from ref. 29; estimates of bottom water temperature are from ref. 16.

destabilized hydrates, the production of free gas pathways within hydrate stability zones, and sediment slumping/landslides that exposed new hydrocarbon conduits (7, 27, 28). In essence, methane hydrates may act as a climate-sensitive valve system for thermogenic hydrocarbons.

We examine gas hydrate stability during three intervals, each marked by different pressure/temperature conditions, to assess the potential for hydrate destabilization and inferred "activation" of petroleum reservoirs (Figs. 1 and 4). Estimates of gas hydrate stability in Fig. 1 and 4 are based on assumptions detailed in the following section. Gas hydrate stability and estimates of changing SBC bottom water temperatures were from refs. 16 and 29.

First, during the Last Glacial Maximum (scenario 1; 18 ka) when bottom water temperatures were 2°C and sea level was ≈120 m below present, gas hydrate stability occurred below ≈420 m in the SBC. During Termination IA (scenario 2; 16–14 ka), when bottom water temperatures had warmed by ≈2°C and sea level had risen by ≈15 m (22), gas hydrate stability existed below 480 m. Finally, in the early Holocene (scenario 3; ≈9 ka), when bottom waters had warmed by an additional 1–2°C and sea level had risen to modern levels, gas hydrate stability was similar to scenario 1, residing below ≈425 m.

Thus, during the Last Glacial Maximum and the Holocene, a combination of specific temperature and sea-level conditions led to similar gas hydrate stability in the SBC (Fig. 1). During the LGM and Holocene (scenarios 1 and 3), almost half of the deep SBC waters were within the gas hydrate stability field; in contrast, during Termination 1A (scenario 2) the majority of the deep SBC was outside of the stability field (Fig. 4). During deglaciation, the depth zone and spatial extent of gas hydrate stability in the basin were reduced, promoting destabilization of existing hydrates. We find that gas hydrates in SBC would have been most susceptible to destabilization during early deglacia-

tion, because of the dominant effect of temperature on gas hydrate stability during this time period.

Gas hydrates and hydrocarbon reservoirs elsewhere along the California coast may have responded similarly. For example, seepage near Point Conception (northwest of SBC) may have contributed to the tar preserved in SBC sediments through transport in the California current (19). Changes in concentrations of petroleum compounds (hopanes) from ODP Site 1016 (3,846 m; on the continental slope offshore Point Conception) correlate with major shifts in climate, with the largest peaks over major deglacial warming during Terminations I and II (13). These hopane peaks were originally interpreted to reflect major reworking of tar from mounds on continental shelves during marine transgression (13). Although sea-level transgression over the shelf may have led to recycling of tar, given the evidence provided by the higher-resolution SBC records, this mechanism now seems unlikely to account for observations from the lower-resolution Site 1016 record (≈5 cm/ky). We interpret the Site 1016 record as strongly supportive evidence for hydrocarbon seepage during deglacial warming and the clear relationship between climate change and marine seepage. The Site 1016 record indicates that direct evidence of hydrocarbon seepage is not limited to restricted basins such as the SBC and is instead a regional-scale process.

Intriguingly, the most significant peak in tar abundance (over Termination IA) overlaps with a distinctive negative $\delta^{13}C$ shift recorded in planktonic foraminifera from these sites (see Fig. 6, which is published as supporting information on the PNAS web site) (16). From 14.6 ka to at least 12 ka, the $\delta^{13}C$ values of *G. bulloides* in MD02-2503 and MD02-2504 shifted from an average of −0.5‰ to −2.0‰, with the most dramatic shift at 14.6 ka. This result provides further evidence of a $\delta^{13}C$-negative source

to the dissolved inorganic carbon pool at this time, consistent with methane seepage.

Modern global methane seepage from marine sources to the atmosphere is estimated to be $\approx$30 Tg/year, reflecting 15% of the natural (nonanthropogenic) sources (3). The tar index and percent tar records demonstrate at least three times more tar in the SBC during the deglaciation relative to the modern. Modern seepage rates from one source in the SBC (Coal Oil Point) average $\approx$0.029 Tg of CH_4 per year[2]; based on this value, we estimate that total methane seepage in SBC is likely >0.10 Tg of CH_4 per year. Thus, methane seepage in this area during the deglaciation may have reached 0.3–0.4 Tg of CH_4 per year. If this change in tar abundance is scaled to estimate global marine methane flux, seepage would have increased to $\approx$90 Tg of CH_4 per year, totaling $\approx$50% of the estimated total methane source during the deglaciation (175–185 Tg of CH_4 per year during the Bølling transition) (30). Such a large estimate would require equivalent and synchronous response from methane seeps around the world, which is unlikely. Although little is known of past global hydrocarbon seepage variability, this work indicates that if similar processes occurred broadly on continental margins, hydrocarbon seepage would represent a significant source of methane to the atmosphere. Thus, these findings suggest that interactions between the hydrocarbon and hydrate reservoirs may increase the amount of available methane that can be transmitted to the ocean and atmosphere during climatic warming.

Methods

Tar in these sediments is readily identified as black-brown, sometimes semitranslucent, and frequently observed in aggregates or accreting on to other particles. The tar index reflects the percentage of sand grains composed of or coated by tar as determined by using stereoscopic light microscopy. Additional information on methods is provided in *Supporting Text*.

- Tar Index 1: Tar is rare. Small flakes accreting to other particles may be observed, but on <10% of the sand-sized grains.
- Tar Index 2: 20% of the grains are composed of and/or covered by tar.
- Tar Index 3: 30% of the grains are composed of and/or covered by tar, rarely observed in aggregates.

- Tar Index 4: 40% of the sand-sized grains are composed of and/or covered by tar; tar/sand aggregates (<1 mm) are present.
- Tar Index 5: 50% of the sand-sized grains are composed of and/or covered by tar; large (>1 mm) tar/sand aggregates present.

For consistency, one investigator determined the tar index for all of the samples in this study and then replicated $\approx$50% of the samples. A second investigator replicated the tar index for $\approx$30 samples to confirm tar abundance estimates and minimize operator error. In total, 10–15% of samples required adjustment by 0.5–1 index point upon replication. Half measures (e.g., 3.5) were used when tar was observed between index points. Sample resolution for the tar index and isotopic analyses is 5–10 cm for most of the core, with two brief high-resolution intervals (1 cm) from 14.7 to 14.2 ka and from 10.8 to 10.6 ka.

For determination of percent tar, a selection of bulk sediment samples (>63 mm fraction) were weighed and then treated in a solution of acetone and dichloromethane (1:1). The tar (in solution) was decanted from the sediments and weighed after solvent removal in a fume hood at room temperature.

Between 10 and 25 *G. bulloides* specimens from the >250-μm fraction were analyzed for stable isotopes. Samples with tar accreting to foraminiferal specimens were avoided for isotopic analyses. Samples for isotopes were cleaned by sonication in methanol and roasted under vacuum for 1 h. Isotopic analyses were conducted by using a 251 light-stable isotope mass spectrometer (Finnigan-MAT, San Jose, CA), with instrumental precision of <0.09‰ for both carbon and oxygen isotopes. All data are expressed as standard δ notation in per mil (‰) relative to PeeDee Belemnite Standard, related by repeated analysis of NBS-19.

1. Chappellaz J, Barnola JM, Raynaud D, Korotkevich YS, Lorius C (1990) *Nature* 345:127–131.
2. Hornafius JS, Quigley D, Luyendyk BP (1999) *J Geophys Res* 104:20703–20711.
3. Kvenvolden K, Rogers BW, Abrams MA, Whelan JK (2005) *Mar Petrol Geol* 22:579–590.
4. Eichhubl P, Greene HG, Naehr T, Maher N (2000) *J Geochem Explor* 69–70:545–549.
5. Orphan VJ, Hinrichs K-U, Ussler W, III, Paull CK, Taylor LT, Sylva SP, Hayes JM, Delong EF (2001) *Appl Environ Microbiol* 67:1922–1934.
6. Richmond WC, Cummings LJ, Hamlin S, Nagaty ME (1979) *Geologic Hazards and Constraints in the Area of OCS Oil and Gas Sale 48, Southern California* (US Geol Survey, Reston, VA), USGS Open File Report No 81-307.
7. Greene HG, Murai LY, Watts P, Maher NA, Fisher MA, Paull CK, Eichhubl P (2006) *Nat Hazards Earth Syst Sci* 6:63–88.
8. Leifer I, Clark JF, Chen RF (2000) *Geophys Res Lett* 27:3711–3714.
9. Hostettler FD, Rosenbauer RJ, Lorenson TD, Dougherty J (2004) *Org Geochem* 35:725–746.
10. Boles JR, Eichhubl P, Garven G, Chen J (2004) *AAPG Bull* 88:947–970.
11. Kennett JP, Cannariato KG, Hendy IL, Behl RJ (2000) *Science* 288:128–133.
12. Hill TM, Kennett JP, Spero HJ (2003) *Mar Micropaleontol* 49:123–138.
13. Yamamoto M, Yamamuro M, Tada R (2000) *Proc Ocean Drilling Program Sci Res* 167:183–194.
14. Hendy IL, Kennett JP, Roark EB, Ingram BL (2002) *Quat Sci Rev* 21:1167–1184.
15. Behl RJ, Kennett JP (1996) *Nature* 379:243–246.
16. Hill T (2004) PhD thesis (Univ of California, Santa Barbara, CA).
17. Orr WL (1986) *Org Geochem* 10:499–516.
18. Crisp PT, Brenner S, Venkatesan MI, Ruth E, Kaplan IR (1979) *Geochim Cosmochim Acta* 44:1791–1801.
19. Lorenson TD, Dougherty JA, Ussler W, III, Paull CK (2003) *Cruise Summary for P-1-02-SC: Acoustic Imaging of Natural Oil and Gas Seeps and Measurement of Dissolved Methane Concentration in Coastal Waters Near Pt Conception, California* (US Geol Survey, Reston, VA), USGS Open File Report No 03-122.
20. Luyendyk B, Kennett J, Clark JF (2005) *Mar Petrol Geol* 22:591–596.
21. Boles JR, Clark JF, Leifer I, Washburn L (2001) *J Geophys Res* 106:27077–27086.
22. Clark PU, McCabe AM, Mix AC, Weaver AJ (2004) *Science* 304:1141–1144.
23. Behl RJ (1995) *Proc Ocean Drilling Program Sci Res* 146:295–308.
24. Kvenvolden KA, McMenamin MA (1980) *US Geol Surv Circ* 825:1–11.
25. Sassen R, Joye S, Sweet ST, DeFreitas DA, Milkov AV, MacDonald IR (1999) *Org Geochem* 30:485–497.
26. Chapman R, Pohlman J, Coffin R, Chanton J, Laphan L (2004) *EOS Trans AGU* 85:361–365.
27. Gorman AR, Holbrook WS, Hornbach MJ, Hackwith KL, Lizarralde D, Pecher I (2002) *Geology* 30:327–330.
28. Paull CK, Brewer PG, Ussler W, III, Peltzer ET, Rehder G, Clague D (2003) *Geo-Mar Lett* 22:198–203.
29. Kvenvolden KA (1993) *Rev Geophys* 31:173–187.
30. Severinghaus J, Brook E (1999) *Science* 286:930–933.